CORROSION SCIENCE AND TECHNOLOGY, Vol.3, No.1(2004), pp.6~13

Effect of Additives on the Stress Corrosion Cracking Behavior of Alloy 600 in High Temperature Caustic Solutions

Do Haeng Hur, Joung Soo Kim, Jae Sun Baek*, and Jung Gu Kim*

Korea Atomic Energy Research Institute,
150 Duckjin-dong, Yuseong-gu, Daejeon 305-353, Korea
**Dept. of Advanced Materials, Sungkyunkwan University,*
300 Chunchun-dong, Suwon 440-746, Korea

The effect of inhibitors on the electrochemical behavior and the stress corrosion cracking resistance of Alloy 600(UNS N06600) was evaluated in 10% sodium hydroxide solution at 315°C. The specimens of a C-ring type for stress corrosion cracking test were polarized at 150 mV above the corrosion potential for 120 hours with and without inhibitors such as titanium oxide, titanium boride and cerium boride. The chemical compositions of the films formed on the crack tip in the C-ring specimens were analyzed using a scanning Auger electron spectroscopy. The cerium boride, the most effective, was observed to decrease the crack propagation rate more than a factor of three compared with that obtained in no inhibitor solution. It was found that the changes of the active-passive transition potentials and the film compositions were related to the resistance to stress corrosion cracking in high temperature caustic solution.

Keywords : *alloy 600, caustic, stress corrosion cracking, inhibitor, cerium boride, titanium compounds, crack tip*

1. Introduction

Alloy 600 (UNS N06600),[1] a typical steam generator tube material of pressurized light water reactors, has experienced various degradations by corrosion such as stress corrosion cracking(SCC) on the inner and outer diameter surface of tube, intergranular attack(IGA) and pitting, and by mechanical damage such as fretting-wear and fatigue. To date of 1999, the original 150 steam generators have been replaced at 51 nuclear units in the world due to tube degradations within their design lives and 20 plants are scheduled to replace their steam generators.[1)]

These tube degradations not only increase the costs for tube inspection, maintenance and repair but also reduce the operation safety and the efficiency of plants. Therefore, the methodologies have been extensively developed to mitigate them. The developed techniques so far can be divided into two categories. The one is a method to improve the material characters by increasing chromium content, by thermal treatment resulting in a chromium carbide decoration with no chromium depletion at grain boundaries and by decreasing the contents of phosphorous and sulfur species segregated along grain boundaries, etc. Thermally treated Alloy 690, an outstanding outcome of these efforts, is now world widely used as tube material of new or replaced steam generators. The other is enhancing the operation environments such as sludge removal by sludge lancing or chemical cleaning,[2),3)] the application of molar ratio control for maintaining crevice pH in a near-neutral range,[4)] boric acid treatment,[5)] plant operation at a reduced temperature, etc. These are very important countermeasures to the degradations because they can be directly applicable to the plants in operation for extending their lives.

In spite of the use of the developed mitigation techniques, secondary side stress corrosion cracking with and without IGA in operating steam generators continues to be the most commonly occurring corrosion mechanism.[1)] Thus, the extensive researches have been performed to develop and qualify corrosion inhibitors. Titanium compounds including titanium dioxide was ones among the inhibitors tested using C-ring[6)] and constant extension rate specimens[7)] and found to be effective in caustic environments. However, their effectiveness, in the case of packed crevices and for arresting cracks, was found to be not so conclusive in model boiler tests.[8),9)] In addition, titanium

1. UNS numbers are listed in *Metals and Alloys in the Unified Numbering System*, published by the Society of Automotive Engineers (SAE) and cosponsored by ASTM.

lactate treatment essentially showed no inhibition to SCC in mildly acidic conditions, resulting in the conclusion that titanium compounds can not be considered as universal efficient inhibitors.[9)]

The objective of this paper is to propose a new inhibitor and to quantify its effectiveness compared with some candidate titanium inhibitors. The stress corrosion cracking tests were performed using C-ring specimens in 10% sodium hydroxide solution at 315℃. The chemical compositions of the passive films formed at the crack tips were also analyzed using an Auger electron spectroscopy.

2. Experimental procedures

2.1 Test material

A single heat of Alloy 600 steam generator tube with a 22.22 mm outer diameter and 1.23 mm wall thickness was used in all tests. The tubing was mill-annealed at 90 0℃ for 10 minute. The chemical composition is given in Table 1.

For anodic polarization measurements, the tubing was longitudinally sectioned into four pieces, flattened and finally cut into a dimension of 5 mm x 10 mm. Stress corrosion cracking tests were performed using C-ring specimens. The specimens were prepared according to ASTM G38-73 and were stressed to a constant deflection of 1.50 mm by means of Alloy 600 bolts and nuts. The C-rings were tested with surfaces in the as-received conditions.

2.2 Test environments

The reference test solution was 10% sodium hydroxide. The inhibitors used in this study were rutile titanium dioxide, anatase titanium dioxide, titanium boride and cerium boride. They were all commercially available reagent grade chemicals and added to the reference solution with 2 g/liter. All tests were conducted at 315℃.

2.3 Polarization test

Polarization tests were conducted in a nickel autoclave with a capacity of 1 liter. The specimens were spot-welded to Alloy 600 lead wire which was then covered with a heat shrinkable polytetrafluoroethylene tube for electrical insulation. The specimens were mechanically polished through 600 grit silicone carbide paper and then ultrasonically cleaned in acetone. A nickel wire and the body of the nickel autoclave were used as a reference electrode and counter electrode, respectively. Before heating the autoclave, the solution was deaerated by pressurizing to 1.38 MPa (200 psi) with 5% hydrogen-95% nitrogen gas followed by a slow depressurization. After this procedure was repeated three times, the mixed gas was continuously purged with a rate of 350 ml/min for 1 hour and was finally pressurized to 1.38 MPa as a cover gas.

Polarization curves were measured from the corrosion potential to the noble potential at a rate of 20 mV/min. The potentials were referred to Ni, if not other notes.

2.4 Stress corrosion cracking test

Three C-ring specimens were used in each test condition to obtain a reliable result. The procedure of the preparation of solution before heating the autoclave was the same as that used in the polarization tests with the exception of the use of a 2 liter nickel autoclave. The specimens were polarized at 150 mV above the corrosion potential for 120 hours. After the tests, the specimens were sectioned through the middle of the C-rings and prepared for metallographic examination in order to measure the crack depth.

2.5 Surface analysis

For the surface analysis of the crack tips, the C-ring specimens with cracks were bent repeatedly until they were split, with care not to touch each crack surface. The Auger depth profiles of the films on the grain facets at the crack tips were obtained by a scanning Auger electron spectroscopy. The analysis was performed using a primary beam energy of 10 kV and a sputtering rate of approximately 80 Angstroms/min on silicone oxide.

Table 1. Chemical Composition of Alloy 600 Tube (weight %)

C	Cr	Fe	Ni	Si	S	Mn	Cu
0.02	15.5	8.4	Bal.	0. 2	0.001	0.2	0.1

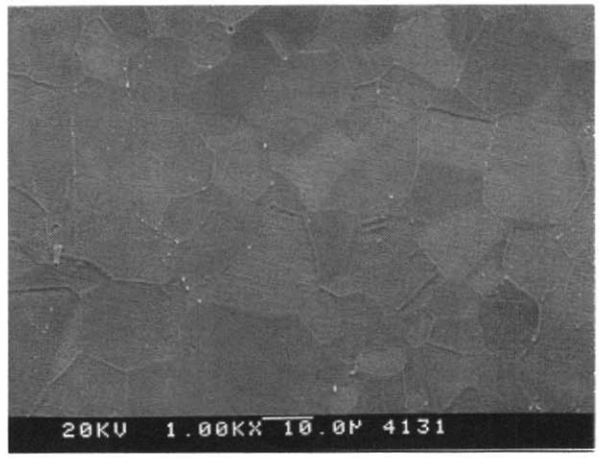

Fig. 1. Microstructure of Alloy 600: Bromine-methanol etch.

3. Results

The details of the microstructure are shown in Fig. 1 after etch in 2% bromine-methanol solution. The microstructure had a fine grain size of about 15 μm. There was sparse inter- and intra-granular chromium carbide precipitation.

3.1 Anodic polarization behavior

Fig. 2 shows anodic polarization curves obtained in 10% NaOH solution at 315°C with and without inhibitors. All curves exhibited the active-passive transition behavior. However, two meaningful changes were recorded with the addition of titanium and cerium compounds. The passive current density decreased in order of TiB_2, anatase TiO_2 and CeB_6. In addition, the active-passive transition potentials moved to the noble direction; 110 mV in the reference solution, 140 mV in TiO_2, 156 mV in TiB_2 and 192 mV in CeB_6 containing solution. There were no other significant differences in the anodic peak current density and corrosion potential.

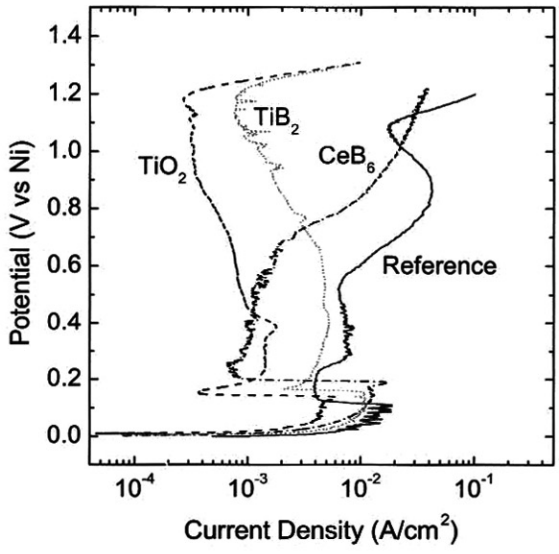

Fig. 2. Effect of inhibitors on the potentiodynamic anodic polarization behavior of Alloy 600 in 10% NaOH at 315°C.

It has been reported that Alloy 600 shows an active-passive transition behavior and its susceptibility to stress corrosion cracking depends on the electrochemical potentials in caustic solutions.[10)-12)] The most susceptible potential is located at the region above the active-passive transition potential. Therefore, it is expected that the increase of the active-passive transition potential by inhibitors enhances the SCC resistance of Alloy 600.

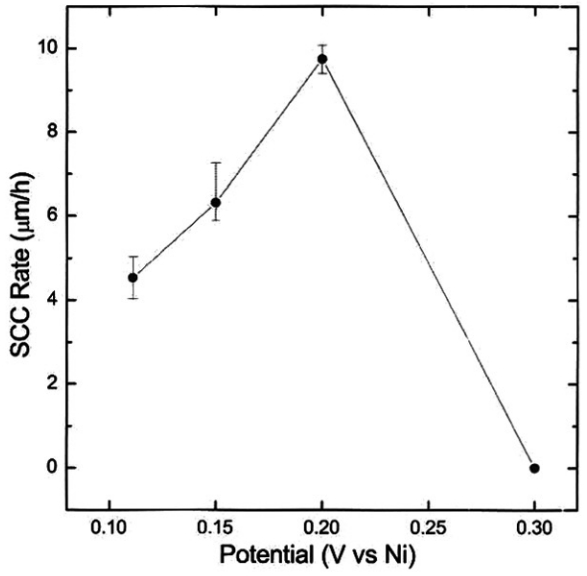

Fig. 3. Crack growth rate versus applied potential for Alloy 600 in 10 wt.% NaOH solution at 315°C.

3.2 Stress corrosion cracking

Fig. 3 shows the effects of inhibitors on the SCC behavior in 10% NaOH solution at 315°C. Stress corrosion cracking was the most susceptible in the reference solution without inhibitors. All the inhibitors tested were found to increase the resistance to SCC of Alloy 600 and CeB_6 among them was the most effective. When the crack propagation rate (CPR) is defined as an average value that the maximum crack depth is divided by the total test time, the CPR was measured to be 6.3 μm/h in the reference solution, 5.5 μm/h in rutile TiO_2, 3.6 μm/h in anatase TiO_2, 2.2 μm/h in TiB_2, and 1.7 μm/h in CeB_6 containing solution. This result indicates that the CPR can be reduced by adding CeB_6 within one third of that in the reference solution. This value with CeB_6 is also much lower than that with anatase TiO_2, a typical inhibitor being used in caustic environments.

It is noteworthy that TiB_2 was the most effective among the titanium compounds. The rutile form of TiO_2 was less effective in inhibiting SCC compared with the anatase form of TiO_2, which is well in accordance with the literature.[6] The cracks initiated at and propagated along grain boundaries regardless of the inhibitors.

3.3 Surface analysis

Fig. 4 shows the outer surface morphology of the C-ring specimens after the SCC tests. The surface films formed on the specimens in the reference solution had grooves along grain boundaries, which probably means that the

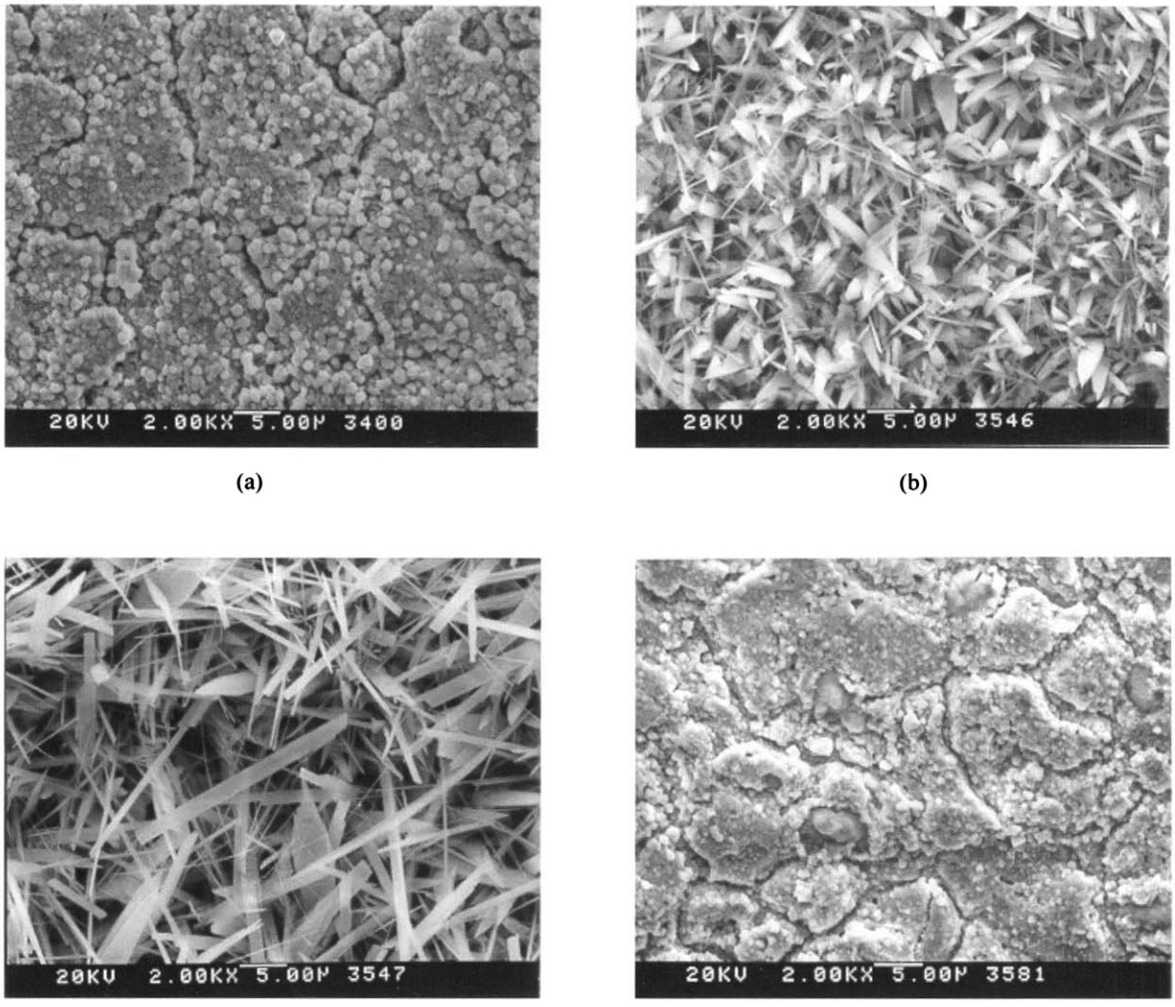

(a) (b)

(c) (d)

Fig. 4. SEM micrographs on the outer diameter surface of the C-ring specimens: (a) pure 10% NaOH, (b) anatase TiO_2, (c) TiB_2 and (c) CeB_6.

preferential corrosion proceeds through grain boundaries, resulting in intergranular stress corrosion cracking.[12] Green colored thick oxide was deposited on the surface of the specimens in the solutions with titanium compounds. It looks like a piece of broken glass in the case of anatase TiO_2, whereas a crushed paper in the case of TiB_2. The deposits were so loose that they were easily removed from the surface during the ultrasonic cleaning process. The film morphology formed in the CeB_6 containing solution was similar to that in the reference solution, but appeared to be denser.

Fig. 5 shows the surface morphology near the crack tips in the C-ring specimens. Cracks are propagated from the upper position to the bottom on the picture. Deformation bands near the crack tip were due to repetitive bending for splitting the specimen. It is clearly shown that

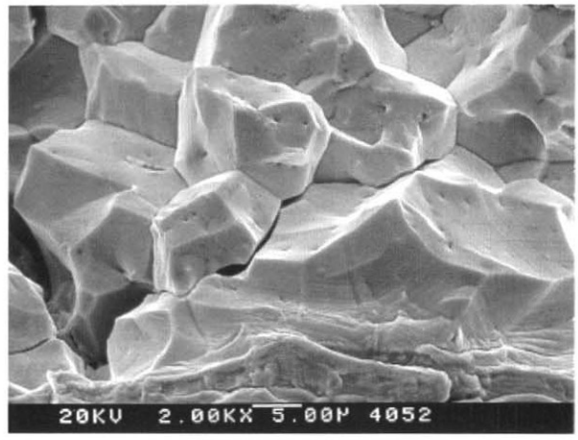

Fig. 5. SEM micrographs around the crack tips of the C-ring specimens exposed to 10% NaOH at 315℃.

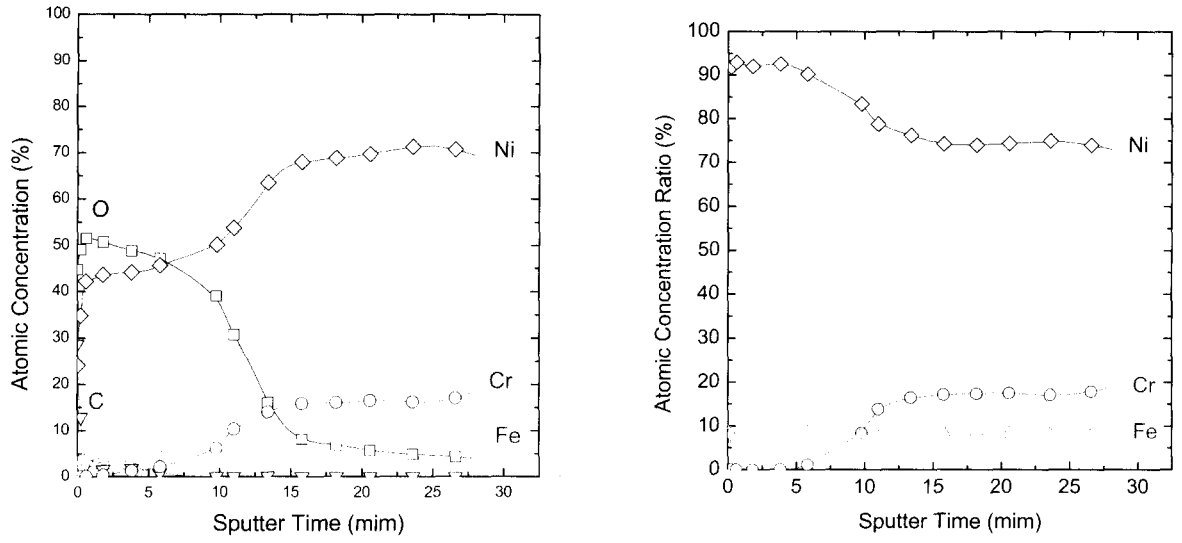

(a) before nomalization (b) after nomalization

Fig. 6. AES depth profiles at the crack tip of the C-ring specimen in 10% NaOH: (a) before and (b) after normalization.

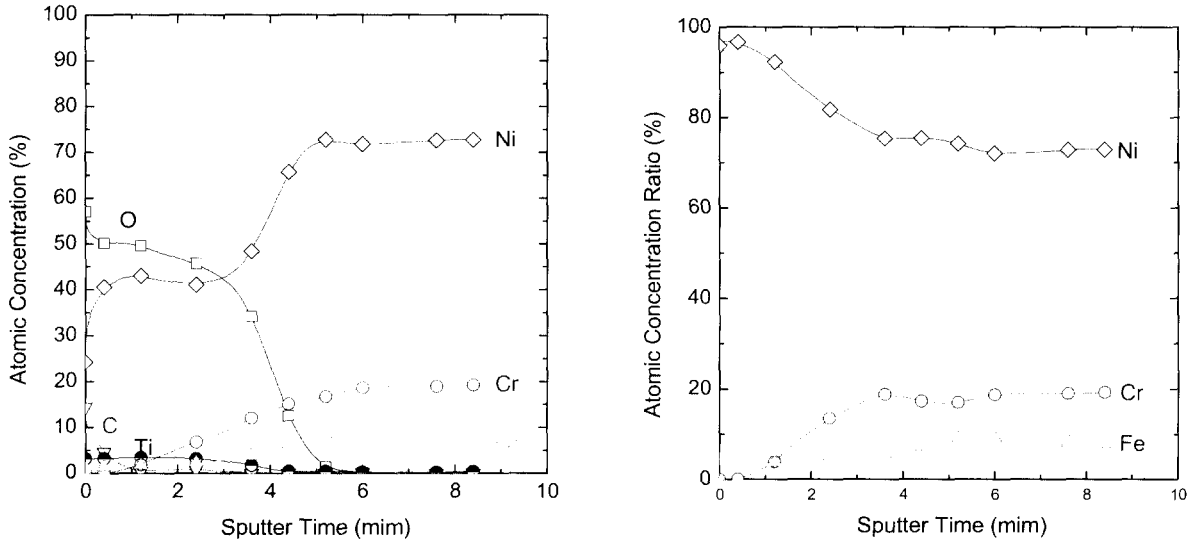

(a) before nomalization (b) after nomalization

Fig. 7. AES depth profiles at the crack tip of the C-ring specimen in 10% NaOH with TiO_2: (a) before and (b) after normalization.

the cracks have the intergranular paths.

The Auger depth profiles of the films were obtained on the grain facets at the crack tips. The results are shown in Figs. 6~8. The profiles that the three major alloy elements are normalized to 100% are also given together. The film formed in the reference solution was a duplex oxide as shown in Fig. 6. The outer layer was composed of a nickel rich oxide with an iron oxide, whereas the inner layer a mixed Ni-Cr-Fe oxide. Chromium in this film was not detected until 5 minutes of sputtering by Argon ions. However, the film formed in the solution with TiO_2, titanium was incorporated in nickel rich oxide, which was a major metallic constituent in the outermost layer, in Fig. 7. It is important to note that the Cr depletion depth in this film was much less than that observed in the film formed in the reference solution. The films exposed to the solution with TiB_2 also were contained titanium and had the Cr depletion

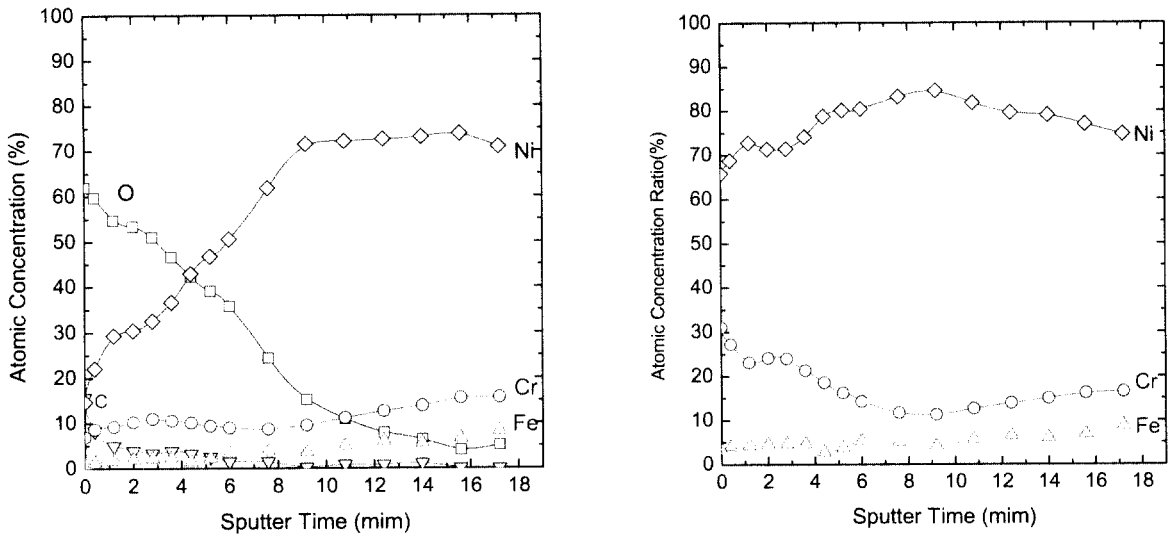

(a) before nomalization (b) after nomalization

Fig. 8. AES depth profiles at the crack tip of the C-ring specimen in 10% NaOH with CeB_6: (a) before and (b) after normalization.

depth like the films formed in the solution with TiO_2. However, boron was not detected.

The drastic changes in the oxide compositions were observed on the depth profiles of the films formed in the solution with CeB_6, as shown in Fig. 8. There was no Cr depletion in the film. Instead, chromium was significantly enriched, up to a content of about 30 atomic percent in the outer layer of the film. However neither Ce nor B was detected in the oxide.

This result was confirmed to be reproducible from the analysis using another specimen. Additionally, the films formed on the outer surface of the C-ring specimens during SCC tests could not be profiled due to charging, regardless of inhibitors.

4. Discussion

The inhibitors shifted the active-passive transition potentials to the noble direction in the polarization curves, specially an increase of 80 mV with the addition of CeB_6. The values of the active-passive transition potentials are well correlated with the effectiveness in inhibiting SCC; the higher the active-passive transition potential, the higher the SCC resistance. It can be rationalized from the fact that SCC of Alloy 600 is most susceptible in the regime above the active-passive transition potential in caustic environments.[11),12)] Since the active-passive transition potential in the reference solution is 110 mV, which is below the applied potential of 150 mV, the cracks propagate fast. However, the active-passive transition potentials in the solutions with inhibitors are above the applied potential of 150 mV, resulting in a decrease of SCC susceptibility. Therefore, the dependence of the CPRs on the electrochemical potential suggests a film rupture type model for the SCC process.

In 10% NaOH solution at 315°C, the approximate values for pH and the standard hydrogen electrode potential are 11.2 and -1.2 V, respectively.[10),13)] Thus, the applied potential of 150 mV to the C-ring specimens corresponds to -1.05 V on the standard hydrogen electrode scale. From the Pourbaix diagrams for Ni, Cr and Fe[14)] in this test conditions, Ni forms a stable NiO film, and Fe forms a Fe_3O_4 oxide or $HFeO_2^-$ species, whereas Cr dissolves as a species of CrO_2^-. Therefore Cr depleted nickel oxide layer having Fe oxide are grown in the 10% NaOH reference solution as shown in Fig. 6.

Selective dissolution of alloying elements would increase the porosity in the film, enhance the transportation of ions through the film and finally deteriorate the stability of the film. It can be, therefore, suggested that inhibition of the selective dissolution of Cr would lead to mitigation of SCC. This is supported by the following result that the addition of titanium compounds decreased the Cr depletion depth and subsequently increased the SCC resistance. In addition, the film with Cr enriched oxide layer minimized the crack growth. It has been also reported that lead would induce SCC by accelerating the selective dissolution of nickel and iron.[15)] Although a Ni-rich dealloyed surface film was formed on the general surface and inside the crack opening, the Cr rich oxide film was

observed at the crack tip by analytical electron microscopy.[13] This subsequently suggests that SCC resistance should be affected by the Cr content of the film.[13]

Ti incorporated in the oxide film possibly decreased the Cr dissolution rate and thus the Cr depletion depth. However, although no Ce and B were detected in the films formed in the solution with CeB_6 within the analysis limit of the Auger spectroscopy, the Cr enriched layer was observed to be formed at the crack tips. Cr has been reported to be enriched in acidic and neutral environments, which can be explained from the Pourbaix diagrams for Ni, Cr and Fe.[14] Boric acid has been used to mitigate secondary side corrosion in caustic environments, of which mechanism is known due to neutralization of the caustic.[8] Judging from the literatures,[7),16] the amount of B in CeB_6 added in this test is so small that the neutralization effect can not be obtained. It is thus reasonable to assume that Cr enrichment would originate from cooperation of Ce with film formed on the surface of Alloy 600, even though, at present, the detail reaction mechanism is not clear. Nevertheless, the fact that the small amount of Ce and CeO_2 alloyed in some iron base alloys drastically enhanced the nucleation Cr_2O_3 and improved the corrosion resistance may become a clue.[17),18]

It should be also noted that the loose and thick deposits fouled the tube surface with the addition of the titanium compounds. Similarly, it was previously reported that the tube surface was covered by ilmenite, a reaction product with titania and magnetite.[8] These deposits may hinder thermal transportation and/or may act as hideout sites for impurities contained in the secondary water. Furthermore, unusually thick or bridged deposits may result in concentrations sufficient to induce corrosion.[4] In reality, the cause of the tube rupture occurred in an operating plant was attributed to IGA/SCC by this mechanism.[19] In contrast, the CeB_6 addition did not induce the loose and thick deposits on the tube surface.

Finally the changes in the SCC resistance of Alloy 600 were well in agreement with the changes in the film character such as the compositions and Cr contents. This result together with the electrochemical behavior again suggests that the SCC mechanism of Alloy 600 in caustic environments be related to a film rupture process.

5. Conclusions

1) The effectiveness of inhibitors in inhibiting SCC of Alloy 600 in 10% NaOH solution at 315°C increased in order of rutile TiO_2, anatase TiO_2, TiB_2 and CeB_6. Especially CeB6 addition decreased the crack propagation rate more than a factor of three compared with that obtained in no inhibitor solution.

2) The active-passive transition potential shifted to the noble direction by the inhibitors; 110 mV in the reference, 140 mV in anatase TiO_2, 156 mV in TiB_2 and 192 mV in CeB_6 containing solution. This resulted in increasing the potential where the cracking was the most susceptible.

3) The Cr depletion depth in the films of the crack tips decreased with the addition of the titanium compounds, moreover the Cr enrichment was observed in the solution with CeB_6. Therefore, it would be essential for inhibition of caustic SCC to find an inhibitor that retards the selective dissolution of Cr, or an inhibitor that enhances the formation of chromium oxide.

4) The changes in film compositions were well correlated with the changes in the SCC resistance, suggesting that the SCC mechanism of Alloy 600 in caustic environments be related to a film rupture process.

Acknowledgements

This work has been carried out as a Steam Generator Materials Project of the Nuclear R&D program supported by the Ministry of Science and Technology.

References

1. J. Benson, Steam Generator Progress Report, Rev. 14, EPRI Report TE-106365-R14 (Palo Alto, CA, EPRI, 1999).
2. D.H. Hur, H.S. Chung, U.C. Kim, *J. Nuclear Materials*, **224**, 179 (1995).
3. D. Schneidmiller and D. Stiteler, Steam Generator Chemical Cleaning Process Development, EPRI Report NP-3009 (Palo Alto, CA, EPRI, 1983).
4. Molar ratio Control Guidelines Committee, PWR Molar Ratio Control Application Guidelines, EPRI Report TR-104811-V1 (Palo Alto, CA, EPRI, 1995).
5. M.J. Partridge, W.S. Zemitis, and J.A. Gorman, Correlation of Secondary-Side IGA/SCC Degradation of Recirculating Steam Generator Tubing With the On-Line Addition of Boric Acid, EPRI Report TR-101010 (Palo Alto, CA, EPRI, 1992).
6. J.B. Lumsden, S.L. Jeanjaquent, J.P.N. Paine, and A. McIlree, "Mechanism and Effectiveness of Inhibitors for SCC in a Caustic Environment", Proc. 7th Int. Symp. on Environmental Degradation of Materials in Nuclear Power Systems-Water Reactors, (Houston, TX, NACE, 1995), p.137.
7. B.P. Miglin, and J.P. Paine, "Slow Strain Rate Testing to Evaluate Inhibitors for Stress Corrosion Cracking of Alloy 600", Proc. 6th Int. Symp. on Environmental Degradation of Materials in Nuclear Power Systems-Water Reactors, (Warrendale, PA, TMS, 1993), p.303.
8. J. Daret, J.P.N. Paine, M.J. Partridge, "Model Boiler

Testing to Evaluate Inhibitors for Caustic Induced Stress Corrosion Cracking of Alloy 600 Tubes", Proc. 7th Int. Symp. on Environmental Degradation of Materials in Nuclear Power Systems-Water Reactors, (Houston, TX, NACE, 1995), p.177.
9. J. Daret, T. Cassagne, and Y. Lefevre, "Secondary Degradation of Steam Generator Tubing: Which Inhibitors for Which Causes? A Review of Model Boiler Test Results", Proc. 8th Int. Symp. on Environmental Degradation of Materials in Nuclear Power Systems-Water Reactors, (LaGrange Park, IL, ANS, 1997), p.100.
10. J.R. Cels, *Corrosion*, **34**, 198 (1978).
11. N. Pessall, G.P Airey, and B.P. Lingenfelter, *Corrosion*, **35**, 100 (1979).
12. R. Bandy, R. Roberge, and D. van Rooyen, *Corrosion*, **41**, 142 (1985).
13. S.A. Shei and W.J. Yang, "Stress Corrosion Crack Tip Microstructure in Nickel-Base Alloys", CORROSION/94, Paper No.154 (1994).
14. P.L. Daniel, and S.L. Harper, Use of Pourbaix Diagrams to Infer Local Pitting Conditions, EPRI Report NP-4831 (Palo Alto, CA, EPRI, 1986).
15. T. Sakai, K. Aoki, T. Shigemitsu, and Y. Kishi, *Corrosion*, **48**, 745 (1992).
16. R.S. Pathania, J.P.N. Panie, and C.E. Shoemaker, "Inhibition of Intergranular Attack and Stress Corrosion Cracking With Boric Acid", Proc. Third Int. Symp. on Environmental Degradation of Materials in Nuclear Power Systems-Water Reactors (Warrendale, PA, The Metallurgical Socierty, 1987), p.511.
17. T.N.Rhys-Jones, H.J. Grabke, and H. Kudielka, *Corrosion Science*, **27**, 49 (1987).
18. K.L. Wang, Q.B. Zhang, M.L. Sun, X.G. Wei, and Y.M. Zhu, *Corrosion Science*, **43**, 255 (2001).
19. P.E. MacDonald, V.N. Shah, L.W. Ward, P.G. Ellison, Steam Generator Tube Failures, NUREG/CR-6365 (U.S. Nuclear Regulatory Commission, 1996), p.105.